Diurnal Covariation in Soil Heat Flux and Net Radiation

JOSEPH A. SANTANELLO JR. AND MARK A. FRIEDL

Department of Geography, Boston University, Boston, Massachusetts

(Manuscript received 10 June 2002, in final form 19 November 2002)

ABSTRACT

Diurnal variation in soil heat flux is a key constraint on the amount of energy available for sensible and latent heating of the lower troposphere. Many studies have demonstrated that soil heat flux G is strongly correlated with net radiation R_n. However, methods to parameterize G based on this relationship typically do not account for the dependency of G on soil properties and ignore asymmetry in the diurnal variation of G relative to R_n. In this paper, the diurnal behavior of G as a function of R_n is examined for sparse cover and bare soil conditions, focusing on patterns of diurnal variation as well as on the effects of soil moisture and soil type. To this end, information from field data is combined with simulations from a multilayer, diffusion-based soil model over a range of soil conditions and vegetation densities. The results show that a relatively simple function can be used to capture the first-order diurnal covariation between G and R_n. Within this framework, soil moisture exerts an important control on this relationship. When soils make the transition from stage-1 (atmosphere limited) to stage-2 (soil limited) evaporation, the ratio of G to R_n tends to increase. Further, soils in stage-2 evaporation exhibit positive G later in the day relative to moist soils. Data from several field experiments show that the amplitude of diurnal surface temperature can be used to predict the magnitude and behavior of G/R_n by integrating the effects of soil type and moisture. Based on these results, a method to estimate G/R_n is proposed that provides a robust representation of G/R_n on hourly timescales for varying soil conditions. This method provides improvement over previous semiempirical treatments for G for which diurnal energy balance closure is required.

1. Introduction

Land surface energy balance (LSEB) models require methods to partition net radiation R_n into fluxes of latent heat λE, sensible heat H, and soil heat G. Although often overlooked, the effect of G is important for predicting surface temperature and influences the partitioning of available energy into sensible and latent heat fluxes (e.g., Deardorff 1978). Because G is typically smaller than H or λE, some studies compute this term as a residual term of the energy balance equation or assume it to be negligible on daily timescales (Kustas et al. 1993).

More common is that G is parameterized as a constant proportion of R_n (i.e., $G = cR_n$) that is fixed for the entire day or period of interest. Recommended values for G/R_n are typically around 0.30 for sparse canopies and range from 0.15 to 0.40 in the literature (Brutsaert 1982; Choudhury 1987; Humes et al. 1994; Kustas and Goodrich 1994). This approach has been employed in numerous energy balance (Mecikalski et al. 1999; Norman et al. 1995, 2000) and hydrologic models (Crawford et al. 2000) and has also been used in association with the force–restore method to predict soil temperature and moisture (Deardorff 1978). On daily or longer timescales, when average daily flux values are of interest, this may be sufficient to obtain energy balance closure.

Many empirical studies have shown that G is unfortunately neither constant nor negligible on diurnal timescales, and it can constitute as much as 50% of R_n for surfaces with sparse canopies (Clothier et al. 1986). Field observations show that G/R_n can range from 0.05 to 0.50 and depends on the time of day, soil moisture and thermal properties, and vegetation amount and height (Kustas et al. 1993). For example, results from Idso et al. (1975) show that G/R_n can range from 0.30 for wet soils to 0.50 for dry soils, and Fuchs and Hadas (1972) and Idso et al. (1975) found considerable asymmetry in G/R_n around solar noon during daytime hours for bare soil. Other studies have confirmed that for bare and sparsely covered soils, G/R_n is at a maximum in midmorning and decreases to zero by late afternoon (Camuffo and Bernardi 1982; Kustas et al. 1998, 2000). As a result, midday values of G/R_n are not representative of the entire diurnal cycle, and ignoring asymmetry in G/R_n about solar noon can lead to underestimation of G in the morning and overestimation of G in the afternoon by up to 50%. These errors will produce corresponding errors in modeled turbulent flux quantities (de

Corresponding author address: Joseph A. Santanello Jr., Department of Geography, Boston University, 675 Commonwealth Ave., 442 Stone Science Bldg., Boston, MA 02215.
E-mail: sntnello@crsa.bu.edu

Bruin and Holtslag 1982; Moran et al. 1994). Therefore, using a constant or negligible value for G/R_n is not appropriate in many situations, and realistic energy balance models need to include these effects.

Previous studies have demonstrated that G/R_n depends on soil properties, vegetation, and time of day, but relatively few efforts have attempted to parameterize and to characterize these relationships for LSEB modeling purposes. Moran et al. (1994), Humes et al. (1994), and Norman et al. (2000) all advocate the need to evaluate the dependence of G/R_n on time of day, soil properties, and vegetation density. Aside from using empirical analyses that are site specific, a more generalized approach for these relationships that incorporates soil and temporal characteristics has not yet been attempted.

The purpose of this study is to use data and results from field experiments combined with simulations using a multilayer land surface model to explore relationships between G/R_n and time of day, soil conditions, and vegetation cover. The paper is structured as follows. First, a summary of the key factors controlling G/R_n is presented in section 2. Section 3 describes the land surface model, including the input fields, soil physics employed, and a validation using field data. Results from simulations of G/R_n are presented in section 4 along with a method to estimate G/R_n for different surface conditions. The method is then applied to several different field datasets in section 5. A discussion of the results, confounding issues, and conclusions follows in section 6.

2. Physical controls on G/R_n

a. Asymmetry in G/R_n

Numerous studies have noted systematic diurnal variation in G/R_n, with well-defined asymmetry about solar noon. For example, the results of Fuchs and Hadas (1972) show a phase shift in the relationship between G and R_n over bare soils, with a midday value of G/R_n (0.30) that is lower than the midmorning maximum (0.37) and higher than afternoon values ($\sim$0.25). This pattern is also reflected in the results of Idso et al. (1975), Clothier et al. (1986), and Kustas et al. (1998, 2000), which together encompass a wide range of conditions.

Recognizing the weakness of using a constant ratio at subdiurnal timescales, Kustas et al. (1998) proposed a piecewise linear function in which G/R_n was different for midday versus early morning and late afternoon periods. This parameterization is symmetric about solar noon and captures the sharp changes in G/R_n early and late in the day, but it neglects the phase shift. In a similar way, Friedl (1996) used a function based on the local solar zenith angle to parameterize diurnal variation in G/R_n.

Analytical treatments for G also support the need to account for the phase shift in G/R_n. For example, under the assumption of periodic forcing, the heat-flow equation can be used to estimate G as a function of time of day (Monteith and Unsworth, 1990):

$$G(0, t) = \frac{\sqrt{2}A(0)k' \sin(\omega t + \pi/4)}{(2\kappa'/\omega)^{0.5}}, \qquad (1)$$

where A is the amplitude of the surface temperature wave, k' and κ' are the soil thermal conductivity and diffusivity, respectively, ω is the period (2π/24 h), and t is time. This expression shows that maximum G occurs 3 h before the maximum surface temperature. In most cases of bare and sparsely covered surfaces, the maximum skin temperature occurs nearly concurrently with maximum net radiation and almost always within 30 min. This method provides a good approximation of diurnal variation in soil heat flux, but it unfortunately is not easily applicable in simple energy budget models because k' and κ' must be known.

b. Soil moisture and texture

The results of Fuchs and Hadas (1972), Idso et al. (1975), and Clothier et al. (1986) all show significant variation in maximum daily values for G/R_n ($\approx$0.05–0.50), depending on the degree of soil wetness. In a similar way, Ogee et al. (2001) examined soil heat fluxes under a forest canopy with significant litter. Although overall fluxes were substantially reduced under these conditions, their data show that the majority of variability in G/R_n on hourly timescales arises from soil moisture differences. This dependence arises from the competing effects of changing evaporation rates and soil thermal conductivity as the soil dries.

The importance of soil type in controlling G/R_n was demonstrated by Cellier et al. (1996), who observed substantial ($>$25%) variation in daily average G/R_n values between a sandy loam and loamy soil with similar moisture and surface characteristics. From a modeling standpoint, soil type determines the hydraulic and thermal properties used to model heat transfer and must be chosen carefully. It is not surprising that Cuenca et al. (1996) show a large range in G and R_n, depending on which soil transfer functions are used. For these reasons, realistic parameterization of G/R_n on hourly timescales depends on the amount of soil moisture and on the soil type, particularly for bare and sparsely vegetated soils.

c. Vegetation

For full canopy cover, G/R_n is generally less than 0.10 with little diurnal variation, in which case a constant midday value for G/R_n works reasonably well regardless of surface conditions (Ogee et al. 2001). In converse, average values for G/R_n over sparse canopies and bare soil can range anywhere from 0.10 to 0.50 (Choudhury 1987), depending on soil type and water content.

Several relationships between vegetation properties and G/R_n have been previously developed using remote

sensing indices (Clothier et al. 1986; Choudhury 1987; Jackson et al. 1987; Kustas and Daughtry 1990; Kustas et al. 1993). For example, using a purely empirical approach, Humes et al. (1994) defined

$$c = 0.29 - 0.16(\rho_{\mathrm{NIR}}/\rho_{\mathrm{RED}}) \quad (2)$$

to estimate G, where $c = G/R_n$ and ρ_{NIR} and ρ_{RED} are the surface reflectance in the near-infrared and red wavelengths, respectively. In a similar vein, Friedl (2002) accounted for attenuation of net radiation by vegetation, using

$$R_S = R_n \exp(-0.5\mathrm{LAI}/\mu), \quad (3)$$

where R_S is the radiation at the soil surface, LAI is the leaf area index, and μ is the cosine of the solar zenith angle. Soil heat flux was then estimated as a fixed proportion of R_S. These approaches provide reasonable estimates of *average midday* values of G/R_n for regions with moderate to high canopy cover. However, such techniques are limited by the confounding influences of soil moisture, soil thermal properties, and, most important, asymmetry in diurnal variation in G relative to R_n (Humes et al. 1994; Moran et al. 1994; Kustas et al. 2000).

3. SHAW-model simulations

To examine patterns of G/R_n across different soil types, vegetation, and moisture conditions, a detailed soil–vegetation–atmosphere transfer model was used. The Simultaneous Heat and Water (SHAW) model is a 1D, multilayer soil and vegetation model that simulates the movement of heat and water through canopy, residue, snow, and soil layers (Flerchinger et al. 1998). This model has been used successfully to simulate land surface energy balance over a wide range of conditions on both hourly and seasonal timescales (Flerchinger et al. 1998; Hymer et al. 2000). The flexible layering and detailed treatment of canopy and soil processes make this model suitable for this study.

Inputs to SHAW include hourly meteorological data, vegetation and soil characteristics, and initial soil temperature and moisture at up to 20 nodes. LSEB closure is obtained by solving for the latent and sensible heat fluxes using standard equations based on Ohm's law, and soil heat flux is calculated according to the diffusion equation constrained by the available energy to the soil as the residual of the energy balance. The soil and vegetation profiles are solved simultaneously using finite-difference approximations and a Newton–Raphson technique, and soil moisture fluxes are computed using a modified form of the Richards equation (Flerchinger et al. 1998). The output of the model includes surface fluxes along with temperature and moisture profiles at user-specified levels.

a. Site description

To test the reliability of model results for the purposes of this study, SHAW simulations were performed using data from the Lucky Hills site of the Monsoon '90 field experiment, which was conducted in the Walnut Gulch watershed in Arizona (Kustas and Goodrich 1994). These measurements provide a reliable dataset for a sparsely (<25% cover) vegetated region that is ideal for this study. Surface and atmospheric data were collected during early and midsummer periods (corresponding to dry and wet seasons, respectively) and were used to initialize and to validate SHAW. The leaf area index was prescribed to be 0.4 for the Lucky Hills site (Flerchinger et al. 1998), which allows the majority of incoming radiation to be intercepted at the soil surface. Soil moisture values, measured at multiple locations and at six discrete depths, were relatively dry in the upper 5 cm (<0.10 m^3 m^{-3}), except immediately following precipitation events. For this work, SHAW was implemented using 20 discrete soil layers down to a 1.5-m depth, 10 of which were located in the top 1 cm to capture rapid drying near the surface that is expected under strong insolation and bare soil conditions (Jackson 1973; Idso et al. 1974; Capehart and Carlson 1997; Santanello and Carlson 2001).

To ensure realistic soil moisture and temperature profiles, SHAW was first spun up for 10 yr using cyclical climatic forcing data from Arizona. This step enables SHAW to become insensitive to initial conditions. Complete (20 layer) profiles for Walnut Gulch were selected based on the spun-up profiles (after model equilibrium was achieved: 2–3 yr) that most closely matched measurements of temperature and moisture profiles at Monsoon '90. The remaining surface parameters and model specifications are described in Flerchinger et al. (1998) and are presented in Table 1.

Initial results from SHAW simulations for Lucky Hills showed systematic overestimation of midday net radiation by 75–100 W m^{-2} for all cloud-free days. Inspection of individual radiation balance terms revealed that SHAW was overestimating downwelling longwave radiation ($L_w\downarrow$), apparently because the default atmospheric emissivity employed within SHAW did not correctly account for the amount of water vapor in the lower atmosphere. To correct this problem, the parameterization described by Brutsaert (1975) for atmospheric emissivity was used, which corrected the apparent overestimation of $L_w\downarrow$ and brought modeled net radiation into good agreement with observed values.

b. SHAW energy-balance simulation results

SHAW was run using forcing data from Monsoon '90 (comprising year days 200–240: late July–August), using an hourly time step. Twenty-minute observations of atmospheric and flux data were aggregated to hourly values using a three-point running average for initiali-

TABLE 1. Surface parameters for the Lucky Hills Monsoon '90 site.

Parameter	Value	Data source
Soil type	Sandy loam	Flerchinger et al. (1998)
Pore size distribution index (b)	4.35	Clapp and Hornberger (1978)
Air-entry potential (ψ_e)	−22.0 cm	Clapp and Hornberger (1978)
Saturated conductivity (K_s)	3.8 cm h^{-1}	Clapp and Hornberger (1978)
Bulk density (ρ)	1350 kg m^{-3}	Clapp and Hornberger (1978)
Saturated soil water content (θ_s)	0.44	Clapp and Hornberger (1978)
Albedo (α)	0.22	Kustas and Goodrich (1994)
Roughness length (z_{0m})	4.0 cm	Menenti and Ritchie (1994)
Vegetation height	50.0 cm	Flerchinger et al. (1998)
Leaf area index	0.4	Flerchinger et al. (1998)

zation and validation purposes. Simulations were performed for the entire 41-day period and for discrete 7- and 3-day periods. Because the primary focus here is on diurnal timescales and there were a limited number of clear-sky days with smooth incoming radiation, each day was also run separately using observed forcing data.

Figure 1a shows simulated hourly fluxes of R_n, H, λE, and G along with measurements for day 220. These results are representative for SHAW simulations under clear-sky conditions at the Lucky Hills site. Figure 1b presents a scatterplot of measured versus simulated fluxes for three combined days (207, 208, 220) along with corresponding R^2 values. The rmse of each flux for these three days was $R_n = 16.35$ W m^{-2}, $H = 22.65$ W m^{-2}, $\lambda E = 27.20$ W m^{-2}, and $G = 27.30$ W m^{-2}, which are within the measurement uncertainties and are comparable to or better than previous studies for the same region (Hymer et al. 2000; Flerchinger et al. 1998). Note that significant precipitation events preceded days 207 and 220 by roughly 2–3 days, and latent heat flux was therefore dominant over sensible heating. These conditions contrast with previous studies of soil heat flux performed in bare soil or sparse-canopy regions where latent heat flux was presumed to be negligible (Ogee et al. 2001; Cellier et al. 1996).

4. Soil heat flux simulations

The simulation results presented above show that SHAW is able to simulate energy balance processes realistically using the Monsoon '90 data. We now use this model to examine relationships between G/R_n and soil type, soil moisture, and vegetation. Using atmospheric and surface conditions for the Lucky Hills site on day 207 (which were representative of clear-sky conditions throughout the period, including days 208 and 220), SHAW simulations were performed for varying soil conditions. To perform these simulations, the initial soil moisture profile was varied from near saturation (volumetric soil moisture $\theta = 0.40$ m^3 m^{-3}) to desiccated conditions ($\theta = 0.05$) over 11 different soil types. Each soil, ranging from clays to sands, was represented independently in SHAW using commonly accepted values for hydraulic and thermal properties (Clapp and Hornberger 1978). The resulting relationships between G/R_n, time of day, soil type, soil moisture content, and vegetation amount were then examined. As part of this analysis, we compare our results against the standard parameterization for G ($=cR_n$) and the parameterization for G suggested by Cellier et al. (1996).

a. Moist soils

Figure 2 shows the diurnal pattern of G/R_n simulated by SHAW for 11 soil types, initialized with near-saturated conditions ($\theta = 0.40$) in the upper 2-cm layer (and gradually wetter below). The decrease in G/R_n after the midmorning maximum is clear, and little variation among soil types is evident. Maximum G/R_n occurs at 0900 LDT, 3 h before maximum incoming net radiation (see Fig. 1a). This peak is 2 h earlier than that predicted by Cellier et al. (1996) but agrees with the empirical results of Kustas et al. (2000, 1998) and Clothier et al. (1986). These results may be approximated in a straightforward fashion, using a function of the form

$$G/R_n = A \cos[2\pi(t + 10\,800)/B], \qquad (4)$$

where A represents the maximum value of G/R_n, B is chosen to minimize the deviation between G/R_n from (4) and results from SHAW by adjusting the phase (or shape of G/R_n), and t is time in seconds relative to solar noon. Applying this equation to the data shown in Fig. 2 and finding the best fit for the times when G is positive yields values of 0.31 and 74 000 s for A and B, respectively. The resulting approximation for G has an rmse of 25.1 W m^{-2} and is plotted in Fig. 2 along with a constant value for G/R_n of 0.20 (rmse = 66.0 W m^{-2}) and the parameterization of Cellier et al. (1996) (rmse = 86.6 W m^{-2}).

Note that if (4) is to be of practical use, it should be relatively insensitive to the exact values of A and B. Varying A by ± 0.05 and B by $\pm 15\,000$ s increases the rmse only slightly (Table 2). Inspection of field data has shown that this range of variability is reasonable for an individual site (see section 5). Thus, there is a substantial margin for error in choosing these values whereby significant improvement over previous methods is still obtained. The matter of prescribing these coefficients is discussed in section 5.

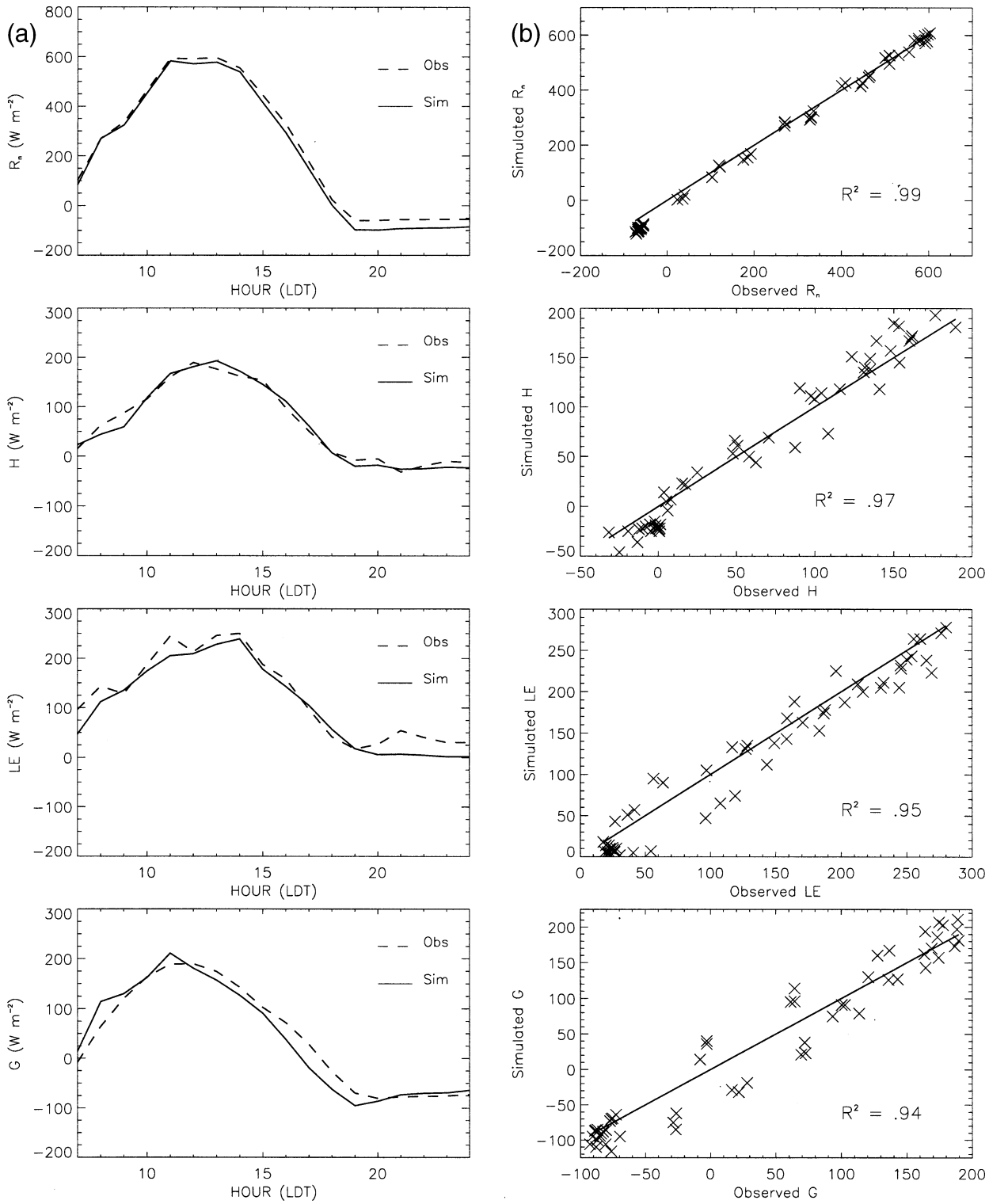

FIG. 1. (a) Time series of simulated vs measured surface fluxes for the Lucky Hills site on yearday 220. (b) Scatterplots of simulated vs measured fluxes for yeardays 207, 208, and 220 along with corresponding R^2 values.

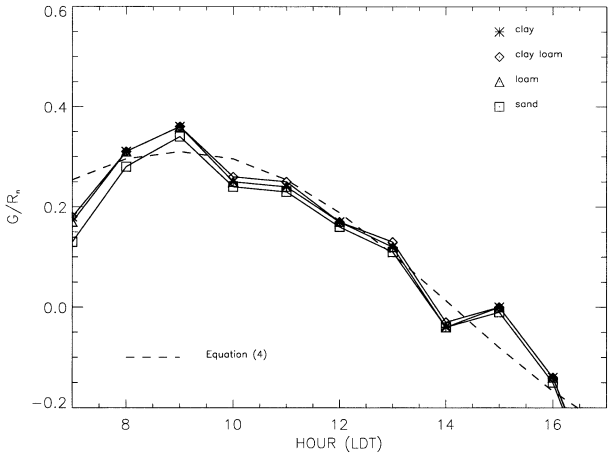

FIG. 2. Time series of simulated G/R_n for the 11 soil types (Clapp and Hornberger 1978), using an initial upper-volumetric soil moisture of 0.40 and average atmospheric forcing from Monsoon '90. Included are estimations from (4), a constant ratio, and that of Cellier et al. (1996).

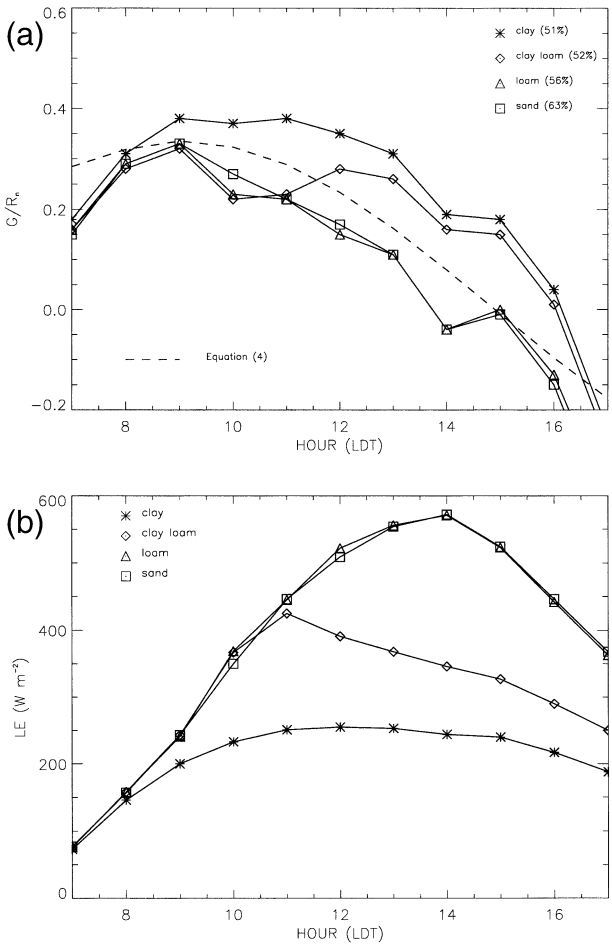

FIG. 3. (a) Same as for Fig. 2, but with initial volumetric soil moisture of 0.25. (b) Latent heat flux for the period simulated in (a) for the 11 soil types.

b. Intermediate moisture

Modeled diurnal variation in G/R_n for four characteristic soil types, each with an initial volumetric soil water content of 0.25, is presented in Fig. 3a along with the percentage saturation for each soil type. Soil type clearly exerts strong control on the modeled diurnal pattern of G/R_n at intermediate soil moisture levels. In particular, clays and clay loams show substantially higher increases in mid- and late-day G/R_n. The best fit of (4) ($A = 0.33$ and $B = 85\,000$ s) to the simulated data in Fig. 3a yields an rmse of 45.7 W m^{-2} in estimating G, versus 61.4 and 77.9 W m^{-2} for the estimates derived from using a constant ratio and the method described by Cellier et al. (1996), respectively.

It is interesting to note that, in Fig. 3a, the clay soils undergo a transition from stage-1 (atmosphere limited) to stage-2 (soil limited) evaporation when their moisture levels drop below 50% of saturation. As this transition occurs, near-surface soil layers are unable to replenish the water lost to evaporation fast enough because of the corresponding decrease in hydraulic conductivity (Idso et al. 1974; van de Griend and Owe 1994; Brutsaert and Chen 1995). Figure 3b shows that a reduction of at least 50% in λE occurs at the same time that the shift in G/R_n takes place for the clays and clay loams. This condition leaves more available energy to heat the soil surface and increases both sensible and soil heat fluxes.

Previous studies have cited thresholds for the transition from stage-1 to stage-2 drying that range between 37% and 50% of saturation and 49% and 66% of field capacity (Capehart and Carlson 1997; Santanello and Carlson 2001; van de Griend and Owe 1994). Because clays have higher saturation values ($\theta \approx 0.48$ by volume), they reach 50% of saturation and their hydraulic conductivity begins to decrease at a higher level of water content than is the case for sands (saturation ~0.40 by volume). They therefore enter stage-2 drying earlier than sandy soils do in model simulations under similar moisture conditions. In reality, sands will tend to dry out more rapidly than clays *during* stage-2 drying, but in this case, with an initial water content of 0.25, the sands have not yet begun the transition.

TABLE 2. Rmse of various fits of (4) to G/R_n simulated for the 11 soil types in Fig. 3a. Also listed for comparison are the errors associated with the constant ratio and Cellier et al. (1996) approximations to G/R_n.

	Best fit	$A + 0.05$	$A - 0.05$	$B + 15\,000$ s	B − 15 000 s	$G = 0.2R_n$	Cellier et al. (1996)
Rmse (W m^{-2})	45.7	55.4	49.4	51.8	55.5	75.6	67.9

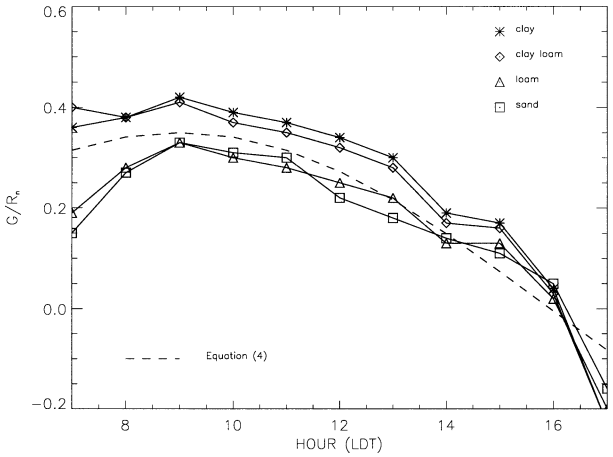

FIG. 4. Same as for Fig. 2, but with initial volumetric soil moisture of 0.05.

Comparison of Figs. 2 and 3a also shows that G becomes negative earlier in the afternoon for moist soils. This occurs because these wet soils possess higher thermal conductivities and evaporation rates, which enable the thermal wave to move more quickly through the soil and reverse the thermal gradient near the surface. In drier soils (exhibiting stage-2 evaporation), the period during which simulated G remains positive increases by 2 h into the late afternoon. This result agrees with the empirical data of Fuchs and Hadas (1972), Idso et al. (1975), Clothier et al. (1986), Betts and Ball (1995), Cuenca et al. (1996), and Cellier et al. (1996).

c. Dry soils

Results from simulations under dry soil conditions (Fig. 4; initial soil water content of 0.05) show that, relative to moist conditions, G/R_n is systematically larger, G does not become negative until after 1600 LDT, and evaporation is negligible (not shown). Because well-dried soils are all in stage-2 or stage-3 (desiccated) drying, parameterization of G can once again be performed independent of soil type. A best fit of (4) to the data shown in Fig. 4 provides values of 0.35 and 100 000 s for A and B, resulting in an rmse of 22.8 W m^{-2} as compared with 50.7 W m^{-2} for a best-fit constant ratio of 0.25 and 32.8 W m^{-2}, using the method of Cellier et al. (1996). As for moist and intermediate soils, (4) improves estimates of soil heat flux under these conditions, even if the soil properties are unknown.

d. Vegetation cover

To assess the sensitivity of diurnal variation in G/R_n to vegetation density, SHAW simulations were performed with LAI assigned values of 0.1, 1.0, 2.5, and 5.0. SHAW was initialized with intermediate (0.25) soil water content, recognizing that some soils experience rapid drying under these conditions. The resulting simulations of G/R_n exhibit two main patterns (Figs. 5a–d). The most obvious effect of increasing vegetation is to decrease the maximum and overall G/R_n values for all soil types. Note, however, that even when LAI = 5.0, G can represent up to 20% of R_n. Second, as vegetation amount increases, differences in G/R_n between dry versus wet soils become smaller.

These results suggest that a single relationship may be sufficient to approximate G/R_n reasonably well for LAI at or above 2.5 for all soil conditions. Surfaces characterized by sparse cover and bare soil, for which maximum and overall values of G/R_n reach more than 3 times those of full cover, exhibit significant variation in G/R_n as a function of soil type and would benefit from parameterizations that account for differences in soil type and moisture.

5. Evaluation using field data

a. Datasets

To ensure that the results presented above are not model or site specific, (4) was evaluated using data from multiple field experiments and was compared with other methods of estimating G. To filter out some of the confounding effects of canopy cover on our results, (3) was used in association with measurements of net radiation data [without the solar zenith angle dependence because (4) already provides for periodic variation], so that the following results examine the behavior of G relative to net radiation estimated at the soil surface R_S.

Betts and Ball (1995) compiled sitewide average flux values from the First International Satellite Land Surface Climatology Project Field Experiment (FIFE; Sellers et al. 1992) for June–September of 1987. Their data, along with measurements of LAI at the site yield values of *average* daily G/R_S of 0.15 and 0.18 for wet and dry conditions, respectively. Figure 6a shows measurements of G/R_S for 10 July 1987, along with a best fit of (4) (A = 0.25, B = 100 000 s) to the data. The rmse of this approximation is 3.55 W m^{-2}, as compared with 15.06 W m^{-2} from Cellier et al. (1996) and 15.02 W m^{-2} using a constant ratio of 0.17. Using the same values for A and B, improvement over previous methods is also observed for multiple dates during each of the intensive field campaigns at FIFE in 1987, which ran from early June through October.

Further evaluations were performed using data from the Monsoon '90 Lucky Hills site and the Hydrological Atmospheric Pilot Experiment in the Sahel (HAPEX—Sahel, Goutorbe et al. 1997). At Monsoon '90, predictions from (4) were compared with observations on year day 207 at the Lucky Hills site (Fig. 6b), using values of 0.41 for A and 120 000 s for B. The resulting rmse of 10.39 W m^{-2} is much lower than that obtained using a constant value of 0.25 (rmse = 27.8 W m^{-2}). For HAPEX—Sahel, values of 0.20 and 90 000 s were estimated for A and B, respectively, and were compared

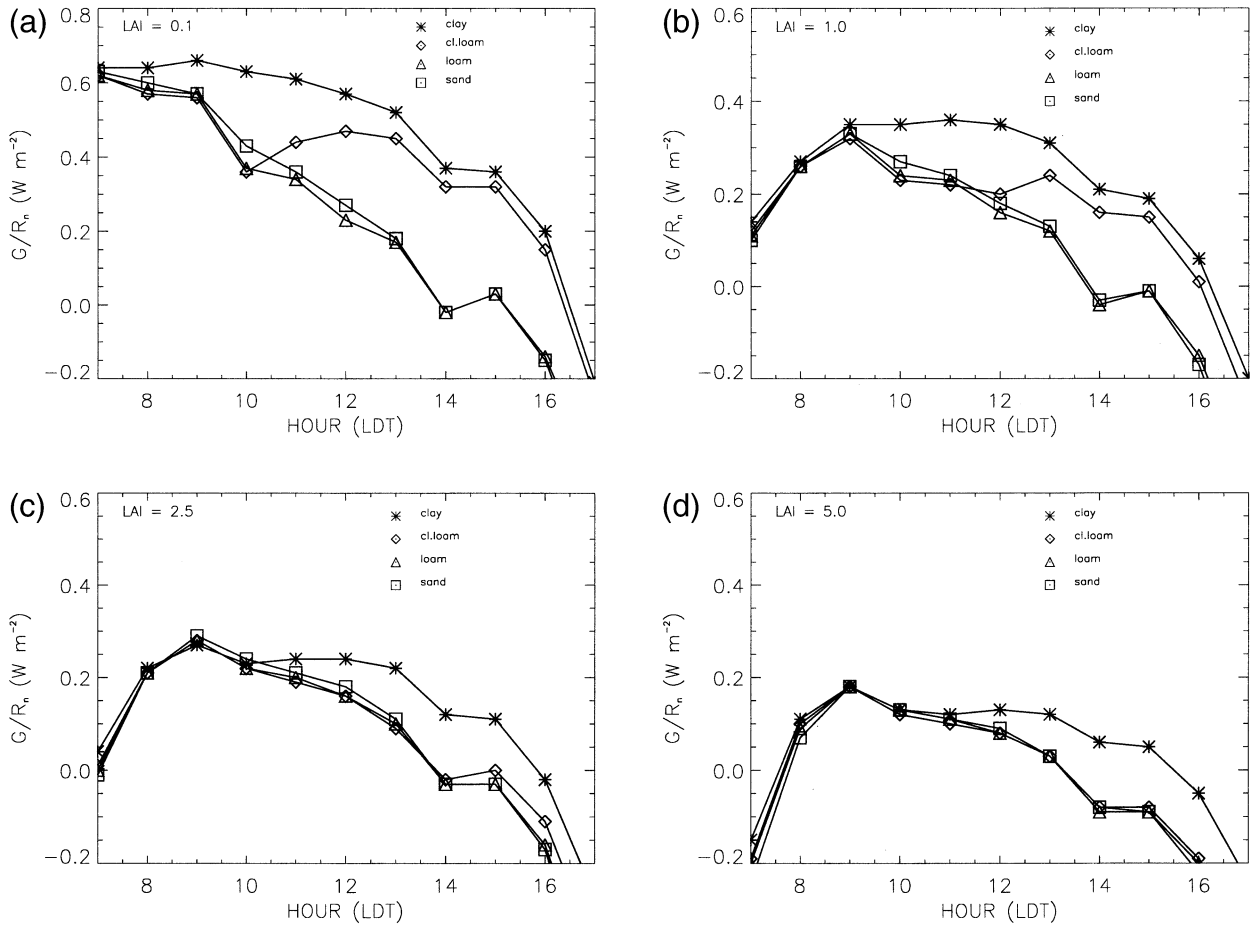

FIG. 5. Time series of G/R_n for four representative soil types, using an initial soil moisture of 0.25 and LAI of (a) 0.10, (b) 1.0, (c) 2.5, and (d) 5.0.

with observations from 8 September 1992 (Fig. 6c). Predictions from (4) provided an rmse of 5.91 W m^{-2}, in contrast to 17.8 W m^{-2} using a constant ratio of 0.15.

b. Specification of A and B

In each of the field datasets examined above, (4) provides a realistic representation of diurnal variability in soil heat flux based on a best fit of the function to the observed data. The values of A and B for a particular location should ideally be assigned based on knowledge of soil type, moisture regimes, and the seasonal dynamics in LAI. These relationships are unfortunately not straightforward because of the confounding effects of variations in soil and canopy properties on soil heat flux.

As a solution, we tested the viability of using diurnal variation in surface temperature to estimate A and B. To be specific, we estimated empirical relationships between the amplitude of diurnal variation in surface skin temperature ΔT_{rad} and both A and B. This change in surface skin temperature, as seen in Fig. 7 for the intermediate-moisture simulations (Figs. 3a,b), is detectable from high-resolution satellite data and could serve as a diagnostic for the maximum value and transition of G/R_n (and λE) that occurs when stage-2 drying begins (Amano and Salvucci 1999; Salvucci 1997).

Figure 8a shows ΔT_{rad} plotted against maximum G/R_n (or A) for a series of randomly selected days from each of the three field experiments examined above. A strong positive relationship is seen between A and ΔT_{rad} ($R^2 = 0.91$). This result suggests that a reasonable estimate for A can be obtained based on surface temperature information. Following the same approach, Fig. 8b shows the relationship between ΔT_{rad} and B, where B was estimated by fitting (4) to data from each of the three field experiments. The results, again, show a positive relationship ($R^2 = 0.56$), with B ranging from 75 000 to 142 000 s. Dry soils exhibit large diurnal variation in surface temperature (an indication of stage-2 evaporation), and higher values for both A and B (and vice versa for moist soils).

Although the R^2 for B is considerably lower than for A, the best-fit line provides an estimate of B that falls within $\pm 15\,000$ s for all but one of the points. Results from the sensitivity analysis discussed in section 4 suggest that this level of uncertainty in B does not introduce

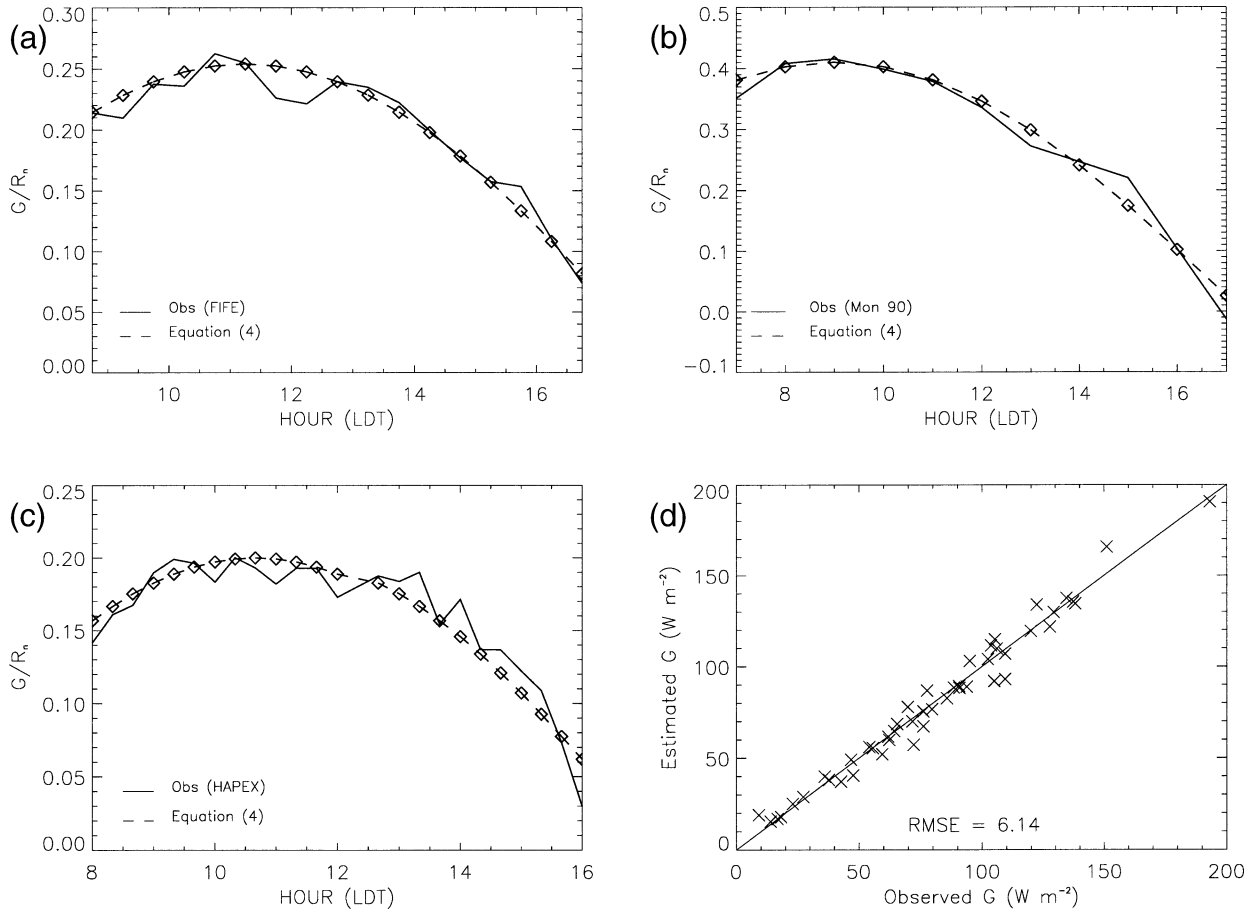

FIG. 6. (a) Time series of G/R_n as measured at FIFE on 10 Jul 1987 and as estimated using (4). (b) Estimated and observed G/R_n at Monsoon '90, yearday 207. (c) Estimated and observed G/R_n at HAPEX—Sahel on 8 Sep 1992. (d) Scatterplot of observed vs estimated G for (a), (b), and (c) with corresponding rmse.

much error into (4) (Table 2). At the same time, a variety of additional factors can confound this relationship. For example, the data from FIFE tend to provide higher values for B at lower magnitudes of ΔT_{rad}, most likely because of vegetation cover. In particular, the FIFE site in 1987 possessed a much higher LAI than the other locations considered, along with a significant thatch layer, both of which decrease and delay heating of the soil surface and soil heat flux in relation to net radiation. This requires an approximation from (4) with a much lower phase (higher B) to capture the diurnal behavior of G.

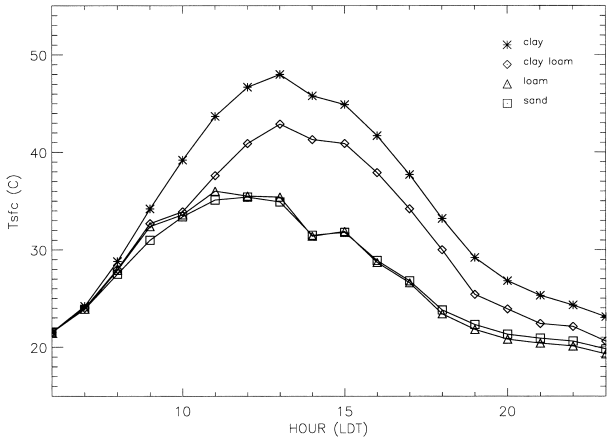

FIG. 7. Simulated surface temperatures for intermediate soil moisture conditions at Monsoon '90 using four representative soil types.

For operational studies, the issue of how to initialize and when to update values for A and B is an important question. For this work, A and B were assigned to be constant for each day. Reinitialization of these constants may be performed as frequently as the available ancillary data allow, depending on the site and timescale of the study. For example, if hourly soil moisture measurements are available, the constants could be adjusted at subdiurnal timescales to allow for changing conditions. However, this type of parameterization would require knowledge, derived from either field measurements or simulation studies, regarding the dependence of A and B on soil moisture for the site of interest. More to the point, unless the site in question is experiencing

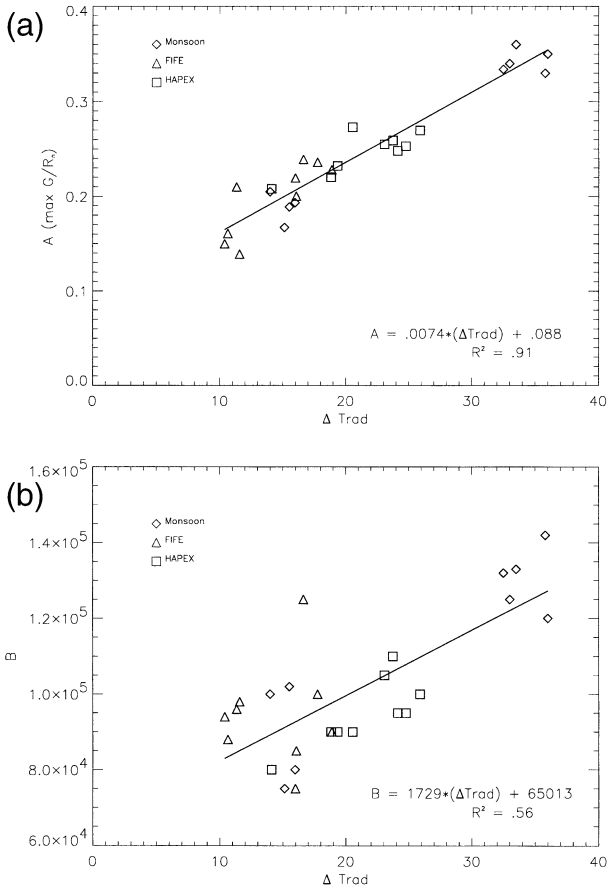

FIG. 8. Scatterplots of the diurnal change in surface radiometric temperature vs (a) maximum G/R_n [A from (4)] and (b) B from (4).

very rapid drying, it is unlikely that adjustments at this timescale will lead to significant improvement in estimates of G.

The results alternatively presented in this paper show that if measurements of surface temperature data are available, then reliable values for A and B should be inferable from measurements of ΔT_{rad}. Overall, the relationships shown in Figs. 8a and 8b provide reasonable estimates for the coefficients in (4) and are robust given that the relationships were observed at three distinct locations with widely varying conditions. At the same time, although the results presented in Fig. 8 are encouraging, these relationships should probably be investigated in more detail to ensure that they are truly robust and applicable. In either case, the SHAW simulation results show that the key factor that needs to be considered in prescribing values for A and B is whether the site in question is in stage-1 or stage-2 drying.

6. Discussion and conclusions

This paper has examined relationships between hourly soil heat flux and net radiation for varying soil and vegetation cover conditions and presents a simple technique to estimate G as a function of R_n. The key advantage of this method is that it captures the diurnal behavior of G/R_n over a range of surface conditions and provides improvement over previous methods of estimating soil heat flux. Although the details and exact tuning depend on the soil type and moisture content, the results show that capturing the phase shift in G/R_n at diurnal timescales is important for regions with sparse vegetation and that tuning this relationship to soil and vegetation conditions can be performed using estimates of LAI and the surface temperature wave, both of which can be obtained from remote sensing.

An important factor pertaining to the use of detailed models to simulate soil heat and moisture dynamics is the behavior of real soils relative to simulations. In SHAW, a single soil type is specified and soil properties are assumed to be vertically constant throughout the soil profile. This description results in a well-behaved drying pattern (defined by the physics of the model). In reality, soil properties can vary greatly within a few meters both horizontally and vertically. Furthermore, parameterization of soil properties based on soil type (e.g., Clapp and Hornberger 1978) makes the simulation results presented here somewhat model specific, and these results could change slightly if a different scheme were used (e.g., van Genuchten 1980). However, the results fall within the range of observations from the various field experiments examined and are therefore considered to be reasonable.

In the same vein, flux measurement error is unavoidable in any field data. Typical uncertainties in flux measurements are generally on the order of 10% or more, and systematic effects such as underestimation of net radiation can contribute bias on the order of 5%. At most, this type of bias would cause a small decrease in the magnitude of A in (4) when fit to the empirical data presented in section 5. However, the ability of (4) to capture the diurnal behavior of G/R_n would not be affected, and measurement error on the order of 5% should have relatively little effect on predictions of G based on this expression. In this context, measurement error is relatively more important when net radiation is small ($R_n < 100$ W m^{-2}), when, for example, an error of 10 W m^{-2} can lead to a 10% error in G. However, because G is typically very small under these conditions, the significance of this type of error will be minimal in terms of its impact on LSEB. Indeed, the smooth form of this equation should decrease variation in modeled values of G relative to measurements, which can exhibit large variations from one time step to the next because of measurement uncertainty.

In terms of the soil physical processes involved, Figs. 3a and 3b show that there are substantial changes in surface fluxes caused by differences in soil moisture and soil hydraulic properties. In contrast to previous studies, which have focused on how this transition influences the surface Bowen ratio, results from this work show that the magnitude and behavior of soil heat flux

TABLE 3. Available energy (W m^{-2}) estimated by each parameterization type for moist, intermediate, and dry soil conditions for the hours when G is positive.

Time	Eq. (4)	Cellier et al. (1996)	$G/R_n = 0.20$	$G = 0$
		Moist soils ($\theta = 0.40$)		
7	84.51	53.71	89.4	127.73
8	176.83	171.52	208.43	297.91
9	261.06	289.72	320.67	458.11
10	345.13	386.89	407.02	581.46
11	440.09	458.25	465.56	665.01
12	535.45	495.86	488.73	698.18
13	623.89	508.06	486.51	695.12
14	609.72	442.81	410.52	586.46
		Intermediate soils ($\theta = 0.25$)		
7	79.67	52.98	88.21	126.01
8	172.62	169.63	206.25	294.64
9	257.54	285.81	316.27	451.82
10	334.69	380.12	399.89	571.27
11	409.68	446.68	453.54	647.91
12	475.38	478.35	471.42	673.46
13	532.71	486.07	465.44	664.91
14	505.43	418.85	388.31	554.73
		Dry soils ($\theta = 0.05$)		
7	80.92	61.06	94.47	188.09
8	187.31	183.77	227.42	284.74
9	284.11	303.26	349.67	437.09
10	363.42	397.75	441.23	551.45
11	427.07	461.95	498.62	623.27
12	471.13	491.11	517.96	647.46
13	501.23	495.98	511.42	639.27
14	449.94	420.81	422.98	528.73

also change based on the stage of soil drying, whereby G increases as the soil dries out and enters stage-2 evaporation. As the evaporation rate decreases, the soil surface heats up and both sensible and soil heat fluxes increase as a result of higher surface temperatures.

One area for which the parameterization for G/R_n presented here holds particular utility is in remote sensing of land surface energy balance (e.g., Kustas et al. 1989). In particular, whereas R_n can be estimated from remote sensing, G is rarely known with good reliability and therefore is commonly parameterized as a fixed proportion of R_n. This kind of treatment can result in significant errors in modeled flux terms. For example, Table 3 presents simulated ''available energy'' ($R_n - G$) based on SHAW and using (4) in association with R_n from SHAW for moist, intermediate, and dry soils. Available energy estimated using a constant ratio of 0.20, the method of Cellier et al. (1996), and by assuming that G is negligible is also included. Note that, in some cases, differences in available energy among the various parameterizations are on the order of 200 W m^{-2}. Because $R_n - G$ is a measure of the energy available for λE and H (and is therefore crucial in determining LSEB closure), these differences cannot be ignored. In addition to incorrectly predicting the diurnal trace of near-surface temperature and humidity, using a constant ratio for G/R_n will lead to overestimation of sensible and latent heating in the early part of the day and vice versa in the afternoon.

It is important to note that the method developed in this paper is not intended to replace LSEB models that employ more sophisticated treatments of G such as numerical solutions to the heat-diffusion equation and multilayer soil models (e.g., Liang et al. 1999), which are physically realistic but are more costly in terms of data, time, and complexity. Rather, the relationships examined in this paper are designed to support energy-balance models and applications in which relatively little site-specific information is available regarding G. In this context, the basic relationships described here should provide improvement to modeled values of G relative to currently available methods.

Acknowledgments. This work was supported by NSF Grant EAR-9725698 and NASA Headquarters under the Earth System Science Fellowship Grant No. NGT5-30405. Technical assistance with SHAW was graciously provided by Gerald Flerchinger. Thanks also are given to Bill Kustas for providing data and to those involved with the Monsoon '90 project. Climate data and guidance on soil moisture spinups were provided by Guido Salvucci. Last, we are grateful for the comments of two anonymous reviewers who provided constructive comments on this paper.

REFERENCES

Amano, E., and G. D. Salvucci, 1999: Detection and use of three signatures of soil-limited evaporation. *Remote Sens. Environ.*, **67,** 108–122.

Betts, A. K., and J. H. Ball, 1995: The FIFE surface diurnal cycle climate. *J. Geophys. Res.*, **100,** 25 679–25 693.

Brutsaert, W., 1975: On a derivable formula for long-wave radiation from clear skies. *Water Resour. Res.*, **11,** 742–744.

——, 1982: *Evaporation into the Atmosphere.* D. Reidel, 299 pp.

——, and D. Chen, 1995: Desorption and the two stages of drying of natural tallgrass prairie. *Water Resour. Res.*, **31,** 1305–1313.

Camuffo, D., and A. Bernardi, 1982: An observational study of heat fluxes and their relationships with net radiation. *Bound-Layer Meteor.*, **23,** 359–368.

Capehart, W. J., and T. N. Carlson, 1997: Decoupling of surface and near-surface soil water content: A remote sensing perspective. *Water Resour. Res.*, **33,** 1383–1395.

Cellier, P., G. Richard, and P. Robin, 1996: Partition of sensible heat fluxes into bare soil and the atmosphere. *Agric. For. Meteor.*, **82,** 245–265.

Choudhury, B. J., 1987: Relationships between vegetation indices, radiation absorption, and net photosynthesis evaluated by a sensitivity analysis. *Remote Sens. Environ.*, **22,** 209–233.

Clapp, R. B., and G. M. Hornberger, 1978: Empirical equations for some soil hydraulic properties. *Water Resour. Res.*, **14,** 601–604.

Clothier, B. E., K. L. Clawson, P. J. Pinter Jr., M. S. Moran, R. J. Reginato, and R. D. Jackson, 1986: Estimation of soil heat flux from net radiation during the growth of alfalfa. *Agric. For. Meteor.*, **37,** 319–329.

Crawford, T. M., D. J. Stensrud, T. N. Carlson, and W. J. Capehart, 2000: Using a soil hydrology model to obtain regionally averaged soil moisture values. *J. Hydrometeor.*, **1,** 353–363.

Cuenca, R. H., M. Ek, and L. Mahrt, 1996: Impact of soil water

property parameterization on atmospheric boundary layer simulation. *J. Geophys. Res.*, **101,** 7269–7277.

Deardorff, J., 1978: Efficient prediction of ground surface temperature and moisture, with inclusion of a layer of vegetation. *J. Geophys. Res.*, **83,** 1889–1903.

de Bruin, H. A. R., and A. A. M. Holtslag, 1982: A simple parameterization of the surface fluxes of sensible and latent heat during daytime compared with the Penman–Monteith concept. *J. Appl. Meteor.*, **21,** 1610–1621.

Flerchinger, G. N., W. P. Kustas, and M. A. Weltz, 1998: Simulating surface energy fluxes and radiometric surface temperatures for two arid vegetation communities using the SHAW model. *J. Appl. Meteor.*, **37,** 449–460.

Friedl, M. A., 1996: Relationships among remotely sensed data, surface energy balance, and area-averaged fluxes over partially vegetated land surfaces. *J. Appl. Meteor.*, **35,** 2091–2103.

——, 2002: Forward and inverse modeling of land surface energy balance using surface temperature measurements. *Remote Sens. Environ.*, **79,** 344–354.

Fuchs, M., and A. Hadas, 1972: The heat flux density in a nonhomogeneous bare loessial soil. *Bound-Layer Meteor.*, **3,** 191–200.

Goutorbe, J. P., and Coauthors, 1997: An overview of HAPEX-Sahel: A study in climate and desertification. *J. Hydrol.*, **189,** 4–17.

Humes, K. S., W. P. Kustas, and M. S. Moran, 1994: Use of remote sensing and reference site measurements to estimate instantaneous surface energy balance components over a semiarid rangeland watershed. *Water Resour. Res.*, **30,** 1363–1373.

Hymer, D. C., M. S. Moran, and T. O. Keefer, 2000: Soil water evaluation using a hydrologic model and calibrated sensor network. *Soil Sci. Soc. Amer. J.*, **64,** 319–326.

Idso, S. B., R. J. Reginato, R. D. Jackson, B. A. Kimball, and F. S. Nakayama, 1974: The three stages of drying of a field soil. *Soil Sci. Soc. Amer. Proc.*, **23,** 183–187.

——, J. K. Aase, and R. D. Jackson, 1975: Net radiation–soil heat flux relations as influenced by soil water content variations. *Bound-Layer Meteor.*, **9,** 113–122.

Jackson, R. D., 1973: Diurnal changes in soil water content during drying. *Soil Sci. Soc. Amer. J.*, 37–55.

——, M. S. Moran, L. W. Gay, and L. H. Raymond, 1987: Evaluating evaporation from field crops using airborne radiometry and ground-based meteorological data. *Irrig. Sci.*, **8,** 81–90.

Kustas, W. P., and C. S. T. Daughtry, 1990: Estimation of the soil heat flux/net radiation ratio from spectral data. *Agric. For. Meteor.*, **49,** 205–233.

——, and D. C. Goodrich, 1994: Preface. *Water Resour. Res.*, **30,** 1211–1225.

——, R. D. Jackson, and G. Asrar, 1989: Estimating surface energy balance components from remotely sensed data. *Theory and Application of Optical Remote Sensing*, G. Asrar, Ed., John Wiley and Sons, 604–627.

——, C. S. T. Daughtry, and P. J. van Oevelen, 1993: Analytical treatment of the relationships between soil heat flux/net radiation ratio and vegetation indices. *Remote Sens. Environ.*, **46,** 319–330.

——, X. Zhan, and T. J. Schmugge, 1998: Combining optical and microwave remote sensing for mapping energy fluxes in a semiarid watershed. *Remote Sens. Environ.*, **64,** 116–131.

——, J. H. Prueger, J. L. Hatfield, K. Ramalingam, and L. E. Hipps, 2000: Variability in soil heat flux from a mesquite dune site. *Agric. For. Meteor.*, **103,** 249–264.

Liang, X., E. F. Wood, and D. P. Lettenmaier, 1999: Modeling ground heat flux in land surface parameterization schemes. *J. Geophys. Res.*, **104,** 9581–9600.

Mecikalski, J. R., G. R. Diak, M. C. Anderson, and J. M. Norman, 1999: Estimating fluxes on continental scales using remotely sensed data in an atmospheric–land exchange model. *J. Appl. Meteor.*, **38,** 1352–1369.

Menenti, M., and J. C. Ritchie, 1994: Estimation of effective aerodynamic roughness of Walnut Gulch watershed with laser altimeter measurements. *Water Resour. Res.*, **30,** 1329–1337.

Monteith, J. L., and M. H. Unsworth, 1990: *Priciples of Environmental Physics.* Edward Arnold, 291 pp.

Moran, M. S., W. P. Kustas, A. Vidal, D. I. Stannard, J. H. Blanford, and W. D. Nichols, 1994: Use of ground-based remotely sensed data for surface energy balance evaluation of a semiarid rangeland. *Water Resour. Res.*, **30,** 1339–1349.

Norman, J. M., W. P. Kustas, and K. S. Humes, 1995: A two-source approach for estimating soil and vegetation energy fluxes from observations of directional radiometric surface temperature. *Agric. For. Meteor.*, **77,** 263–293.

——, ——, J. H. Prueger, and G. R. Diak, 2000: Surface flux estimation using radiometric temperature: A dual-temperature-difference method to minimize measurement errors. *Water Resour. Res.*, **36,** 2263–2274.

Ogee, J., E. Lamaud, Y. Brunet, P. Berbigier, and J. M. Bonnefond, 2001: A long-term study of soil heat flux under a forest canopy. *Agric. For. Meteor.*, **106,** 173–186.

Salvucci, G. D., 1997: Soil and moisture independent estimation of stage-two evaporation from potential evaporation and albedo or surface temperature. *Water Resour. Res.*, **33,** 111–122.

Santanello, J. A., Jr., and T. N. Carlson, 2001: Mesoscale simulation of rapid soil drying and its implications for predicting daytime temperature. *J. Hydrometeor.*, **2,** 71–88.

Sellers, P. J., F. G. Hall, G. Asrar, D. E. Strebel, and R. E. Murphy, 1992: An overview of the First International Satellite Land Surface Climatology Project (ISLSCP) Field Experiment (FIFE). *J. Geophys. Res.*, **97,** 18 345–18 372.

van de Griend, A. A., and M. Owe, 1994: Bare soil surface resistance to evaporation by vapor diffusion under semiarid conditions. *Water Resour. Res.*, **30,** 181–188.

van Genuchten, M. T., 1980: A closed-form equation for predicting the hydraulic conductivity of unsaturated soils. *Soil Sci. Soc. Amer. J.*, **44,** 892–898.